

# Linear, diatomic crystal: single-electron states and large-radius excitons

Vadym M. Adamyan\*, Oleksii A. Smyrnov†

*Department of Theoretical Physics, Odessa I. I. Mechnikov National University,  
2 Dvoryanskaya St., Odessa 65026, Ukraine*

April 2, 2008

## Abstract

The large-radius exciton spectrum in a linear crystal with two atoms in the unit cell was obtained using the single-electron eigenfunctions and the band structure, which were found by the zero-range potential (ZRP) method. The ground-state exciton binding energies for the crystal in vacuum appeared to be larger than the corresponding energy gaps for any set of the crystal parameters.

PACS number(s): 73.22.Dj, 73.22.Lp, 71.35.Cc

## 1 Introduction

The study of the quasio-one-dimensional semiconductors with the cylindrical symmetry became an urgent problem as soon as investigations of semiconducting nanotubes had been launched. One of the most important trends of research in this field is the study of optical spectra of single-walled carbon nanotubes (SWCNTs), which, as it is shown in [1]-[5], should include the exciton contributions. Evidently, the quasio-one-dimensional large-radius exciton problem can be reduced to the 1D system of two quasi-particles with the potential having Coulomb attraction tail. Due to the parity of the interaction potential the exciton states should split into the odd and even series. In [6] we show that for the bare and screened Coulomb interaction potentials the binding energy of even excitons in the ground state well exceeds the energy gap (in the same work we also discuss the factors, which prevent the collapse of single-electron states in isolated semiconducting SWCNTs). But the electron-hole (e-h) interaction potential and so the corresponding exciton binding energies may noticeably depend on the electron and hole charge distributions. So it is worth to ascertain whether the effect of seeming instability of single-electron states near the gap is inherent to the all quasio-one-dimensional semiconductors in vacuum or it maybe takes place only in SWCNTs for the specific localization of electrons (holes) at their surface and weak screening by the bound electrons. That is why we consider here the simplest model of the quasio-one-dimensional semiconductor with the cylindrical symmetry, namely the linear crystal with two atoms in the unit cell. The electrons (holes) in this crystal are simply localized at its axis.

The aim of this work is only a qualitative analysis of the mentioned effect, so we can use the linear crystal parameters (the electron bare mass, lattice parameters) taken from works on nanotubes [7], [8]. The results of [7] and [8] on the band structure and single-electron states in SWCNTs, obtained within the framework of the zero-range potential (ZRP) method [9], are in good accordance with the experimental data (the interband optical absorption). Therefore, we also apply here this method to the mentioned linear crystal (see section 2). In section 3 we obtain the large-radius exciton interaction potential and its spectrum for the linear crystal in vacuum. In the same section we also get the e-h interaction potential screened by the crystal bound electrons. All these data are used in section 4, where we present results of calculations for the crystal with different lattice periods (it also means different band structures). As it turns out, the binding energy of even excitons in the ground state well exceeds the energy gap for the linear crystal in vacuum and the screening by the crystal bound electrons is negligible. Hence, the mentioned instability effect takes place not only for SWCNTs, but in this simplest case too, and, most likely, for the all quasio-one-dimensional isolated semiconductors in vacuum.

---

\*E-mail: vadamyam@paco.net

†E-mail: smyrnov@onu.edu.ua

## 2 Single-electron band structure and eigenfunctions of band electrons

Within the framework of the zero-range potential method [9] it is assumed that the electron wave functions in the linear crystal satisfy the Schrödinger equation for a free particle except for the points of ions localization. Thus, we can seek them in the following form:

$$\psi(\rho_n^A, \rho_n^B) = \sum_{n=-\infty}^{\infty} A_n \frac{\exp(-\kappa \rho_n^A)}{\rho_n^A} + \sum_{n=-\infty}^{\infty} B_n \frac{\exp(-\kappa \rho_n^B)}{\rho_n^B}, \quad (2.1)$$

where indices A and B denote two monatomic sublattices of the diatomic lattice,  $\rho_n^A = |\mathbf{r} - \mathbf{r}_n^A|$  and  $\rho_n^B = |\mathbf{r} - \mathbf{r}_n^B|$ ,  $n$  numbers all the sublattices points,  $\kappa = \sqrt{2m_b|E|}/\hbar$ ,  $E < 0$  is the electron energy and  $m_b \simeq 0.415 m_e$  is the bare mass, which was chosen according to works [7], [8], where it was the universal fitting parameter for all SWCNTs. One can take infinite limits for the series in (2.1) even for the finite crystal, because terms of these series decrease exponentially with increasing of  $n$ .

According to the zero-range potential method the interaction between electron and atoms (ions) of the crystal is described by the following boundary conditions imposed on the wave functions (2.1) at the all sublattices points:

$$\lim_{\rho_l^A \rightarrow 0} \left\{ \frac{d}{d\rho_l^A} (\rho_l^A \psi)(\mathbf{r}) + \alpha (\rho_l^A \psi)(\mathbf{r}) \right\} = 0 \quad (2.2)$$

and

$$\lim_{\rho_l^B \rightarrow 0} \left\{ \frac{d}{d\rho_l^B} (\rho_l^B \psi)(\mathbf{r}) + \alpha (\rho_l^B \psi)(\mathbf{r}) \right\} = 0, \quad (2.3)$$

where  $\alpha$  is the interaction constant, which corresponds to the ZRP depth  $2\pi/\alpha$ . We put  $\alpha$  to be equal  $\sqrt{2m_b|E_{\text{ion}}|}/\hbar$ , where  $E_{\text{ion}}$  is the ionization energy of an isolated atom.

Further we suppose that the linear crystal lies along the  $z$ -axis, thus  $\mathbf{r}_n^A = nd\mathbf{e}_z$  and  $\mathbf{r}_n^B = (nd + a)\mathbf{e}_z$ , where  $\mathbf{e}_z$  is the  $z$ -axis unit vector,  $a$  is the distance between atoms in the unit cell of the crystal and  $d > 2a$  is the distance between the neighbor atoms in each sublattice. Note, that  $d = 2a$  corresponds to the metallic monatomic crystal and for the case  $d < 2a$  the smallest distance between atoms in the crystal is  $d - a < a$ .

Substituting (2.1) to (2.2) and (2.3) and applying the Bloch theorem ( $A_n = A \exp(iqdn)$ ,  $B_n = B \exp(iqdn)$ ,  $q$  is the electron quasi-momentum) we get two equations for amplitudes  $A, B$ :

$$\begin{cases} AQ_1 + BQ_2 = 0, \\ AQ_2^* + BQ_1 = 0, \end{cases} \quad (2.4)$$

where

$$Q_1(\kappa, q) = \alpha - \frac{1}{d} \ln(2[\cosh \kappa d - \cos qd]), \quad (2.5)$$

$$Q_2(\kappa, q) = \sum_{n=-\infty}^{\infty} \frac{\exp(-\kappa|nd + a| + iqnd)}{|nd + a|}. \quad (2.6)$$

Setting  $d = ja$ :

$$Q_2(\kappa, q) = \frac{1}{a} \int_0^1 \left( \frac{\exp[-\kappa a]}{1 - x^j \exp[d(iq - \kappa)]} + \frac{x^{j-2} \exp[\kappa a]}{\exp[d(iq + \kappa)] - x^j} \right) dx \quad (2.7)$$

for each real  $j > 2$ .

From (2.4) we get two equations, which define the band structure of the crystal:

$$Q_1(\kappa_1, q) - |Q_2(\kappa_1, q)| = 0, \quad (2.8)$$

$$Q_1(\kappa_2, q) + |Q_2(\kappa_2, q)| = 0. \quad (2.9)$$

Equation (2.8) defines the conduction band and equation (2.9) defines the valence band (see section 4, figure 1). So the electron and hole effective masses can be simply obtained from (2.8) and (2.9), respectively.

Further, using the Hilbert identity for Green's function of the 3D Helmholtz equation, we obtain the normalized wave functions (2.1):

$$\psi_{\kappa,q}(\mathbf{r}) = \frac{A(\kappa,q)}{\sqrt{L}} \left( \sum_{n=-\infty}^{\infty} \frac{\exp(-\kappa|\mathbf{r} - nd\mathbf{e}_z| + iqnd)}{|\mathbf{r} - nd\mathbf{e}_z|} - \frac{Q_1}{Q_2} \sum_{n=-\infty}^{\infty} \frac{\exp(-\kappa|\mathbf{r} - (nd+a)\mathbf{e}_z| + iqnd)}{|\mathbf{r} - (nd+a)\mathbf{e}_z|} \right), \quad (2.10)$$

where  $L$  is the crystal length and  $A(\kappa,q)$  is the normalization factor:

$$A(\kappa,q) = \frac{1}{2} \left( \frac{\kappa d \cosh \kappa d - \cos qd}{\pi \sinh \kappa d - \Re y} \right)^{1/2},$$

and

$$y = \frac{Q_1}{Q_2} (\exp[-iqd] \sinh \kappa a + \sinh \kappa[d-a]).$$

### 3 Exciton spectrum and eigenfunctions. Bare and screened e-h interaction

As it was shown in [6], within the framework of the so-called long-wave approximation the wave equation for the envelope function  $\phi$  of a large-radius exciton in quasio-one-dimensional semiconductor with longitudinal period  $d$  is reduced to the following 1D Schrödinger equation:

$$-\frac{\hbar^2}{2\mu} \phi''(z) + V(z)\phi(z) = \mathcal{E}\phi(z), \quad \mathcal{E} = E_{\text{exc}} - E_g, \quad -\infty < z < \infty, \quad (3.1)$$

with the exciton reduced effective mass  $\mu$  and the e-h interaction potential

$$V(z) = - \int_{\mathbf{E}_3^d} \int_{\mathbf{E}_3^d} \frac{e^2}{((x_1 - x_2)^2 + (y_1 - y_2)^2 + (z + z_1 - z_2)^2)^{1/2}} \times |u_{c;\kappa,\pi/d}(\mathbf{r}_1)|^2 |u_{v;\kappa,\pi/d}(\mathbf{r}_2)|^2 d\mathbf{r}_1 d\mathbf{r}_2, \\ \mathbf{E}_3^d = \mathbf{E}_2 \times (0 < z < d).$$

Here  $u_{c,v;\kappa,q}(\mathbf{r})$  are the Bloch amplitudes of the Bloch wave functions  $\psi_{c,v;\kappa,q}(\mathbf{r}) = \exp(iqz)u_{c,v;\kappa,q}(\mathbf{r})$  of the conduction and valence band electrons of the linear crystal, respectively. Using the actual localization of the Bloch amplitudes at the crystal axis, after several Fourier transformations and simplifications we adduce the e-h interaction potential to the following form:

$$V_{r_1,r_2}(z) = -\frac{4e^2 r_1^2}{r_2 d^2} \int_0^\infty \frac{J_1(k) J_1(kr_2/r_1)}{k^4} \left( \frac{k}{r_1} (|d-z| + |d+z| - 2|z|) + \exp\left[-\frac{k}{r_1}|d-z|\right] + \exp\left[-\frac{k}{r_1}|d+z|\right] - 2 \exp\left[-\frac{k}{r_1}|z|\right] \right) dk, \quad (3.2)$$

where  $J$  is the Bessel function of the first kind and  $r_1$  ( $r_2$ ) is the radius of the electron (hole) wave functions transverse localization,

$$r_{1,2} = \left( 2 \int_{\mathbf{E}_2} r_{2D}^2 \int_0^L |u_{c,v;\kappa,q}(z, \mathbf{r}_{2D})|^2 dz d\mathbf{r}_{2D} \right)^{1/2},$$

where  $\mathbf{r}_{2D}$  is the transverse component of the radius-vector,  $q = \pi/d$  and  $\kappa = \kappa_{1,2}(\pi/d)$  correspond to the conduction and valence bands edges at the energy gap (according to (2.8) and (2.9), respectively). Equation (3.1) with the potential given by (3.2) defines the spectrum of large-radius exciton in the linear, diatomic crystal if the screening effect by the crystal electrons is ignored. Actually, the screening of the potential (3.2) by the band electrons is insignificant.

Indeed, following the Lindhard method (so-called RPA), to obtain the e-h interaction potential  $\varphi(\mathbf{r})$ , screened by the electrons of linear lattice, let us consider the Poisson equation:

$$-\Delta\varphi(\mathbf{r}) = 4\pi(\rho^{\text{ext}}(\mathbf{r}) + \rho^{\text{ind}}(\mathbf{r})), \quad (3.3)$$

where  $\mathbf{r}$  is the radius-vector,  $\rho^{\text{ext}}(\mathbf{r})$  is the density of extraneous charge and  $\rho^{\text{ind}}(\mathbf{r})$  is the charge density induced by the extraneous charge.

By (3.3) the screened e-h interaction potential may be written as:

$$\varphi(\mathbf{r}) = 4\pi \int_{\mathbb{E}_3} (\rho^{\text{ext}}(\mathbf{r}') + \rho^{\text{ind}}(\mathbf{r}')) G(\mathbf{r}, \mathbf{r}') d\mathbf{r}', \quad (3.4)$$

where  $G(\mathbf{r}, \mathbf{r}') = 1/(4\pi|\mathbf{r} - \mathbf{r}'|)$  is Green's function of the 3D Poisson equation.

Let  $E^0(q)$  and  $\psi_{\kappa,q}^0(\mathbf{r}) = \exp(iqz)u_{\kappa,q}^0(\mathbf{r})$  be the band energies and corresponding Bloch wave functions of the crystal electrons and  $E(q)$ ,  $\psi_{\kappa,q}(\mathbf{r})$  be those in the presence of the extraneous charge. Then

$$\rho^{\text{ind}}(\mathbf{r}) = -e \sum_q [f(E(q))|\psi_{\kappa,q}(\mathbf{r})|^2 - f(E^0(q))|\psi_{\kappa,q}^0(\mathbf{r})|^2], \quad (3.5)$$

where  $f$  is the Fermi-Dirac function. Using the transverse localization of the Bloch wave functions near the crystal axis, we get in the linear in  $\varphi$  approximation:

$$\begin{aligned} \rho^{\text{ind}}(z', \mathbf{r}'_{2D}) = & -e^2 \sum_{q,q'} \frac{1}{E_{g;q,q'}} \int_0^L \int_{\mathbb{E}_2} u_{v;\kappa_2,q'}(z, \mathbf{r}_{2D}) u_{c;\kappa_1,q}^*(z, \mathbf{r}_{2D}) d\mathbf{r}_{2D} \varphi(z) \exp[iz(q' - q)] dz \\ & \times u_{v;\kappa_2,q'}^*(z', \mathbf{r}'_{2D}) u_{c;\kappa_1,q}(z', \mathbf{r}'_{2D}) \exp[iz'(q - q')], \end{aligned} \quad (3.6)$$

where  $E_{g;q,q'} = E_c(q) - E_v(q')$ . Here and further  $\varphi(z)$  is the e-h interaction potential averaged in  $\mathbb{E}_2$  over the region of the Bloch wave functions transverse localization and over the lattice period  $d$  along the crystal axis.

Due to the periodicity of the Bloch amplitudes  $\rho^{\text{ind}}$  may be written as:

$$\rho^{\text{ind}}(\mathbf{r}') = -\frac{e^2 N}{L} \sum_{q,q'} \frac{C(q, q'; d)}{E_{g;q,q'}} \varphi(q - q') u_{v;\kappa_2,q'}^*(\mathbf{r}') u_{c;\kappa_1,q}(\mathbf{r}') \exp[iz'(q - q')], \quad (3.7)$$

where

$$C(q, q'; d) = \int_0^d \int_{\mathbb{E}_2} u_{c;\kappa_1,q}^*(z, \mathbf{r}_{2D}) u_{v;\kappa_2,q'}(z, \mathbf{r}_{2D}) d\mathbf{r}_{2D} dz$$

and  $N$  is the number of unit cells in the crystal.

Further, after several transformations we obtain from (3.4) and (3.7) the one-dimensional Fourier transform of the potential  $\varphi$ :

$$\begin{aligned} \varphi(k) &= \frac{\varphi_0(k)}{\varepsilon(k)}, \\ \varepsilon(k) &= 1 + \frac{e^2 N^2}{2\pi^2} \int_{-\pi/d}^{\pi/d} \frac{|C(q, q - k; d)|^2}{E_{g;q,q-k}} dq \tilde{K}_0(k) \frac{2 \sin(kd/2)}{kd}, \end{aligned} \quad (3.8)$$

where  $\varphi_0$  is the Fourier transform of the averaged electrostatic potential induced by  $\rho^{\text{ext}}$  and  $\tilde{K}_0(k)$  is the modified Bessel function of the second kind averaged over  $\mathbf{r}_{2D}$  and  $\mathbf{r}'_{2D}$  in the region of the Bloch wave functions transverse localization in  $\mathbb{E}_2$ , namely

$$\begin{aligned} \tilde{K}_0(k) &= \frac{1}{(\pi r_1 r_2)^2} \int_{\mathbb{E}_2^{r_1}} \int_{\mathbb{E}_2^{r_2}} K_0(|k||\mathbf{r}_{2D} - \mathbf{r}'_{2D}|) d\mathbf{r}_{2D} d\mathbf{r}'_{2D}, \\ \mathbb{E}_2^{r_i} &= (0 \leq r_{2D} \leq r_i) \times (0 \leq \beta \leq 2\pi). \end{aligned}$$

In the long-wave limit we get:

$$|C(q, q - k; d)|_{k \rightarrow 0}^2 \approx |U(q; d)|^2 k^2, \quad (3.9)$$

$$U(q; d) = \int_0^d \int_{\mathbf{E}_2} u_{c; \kappa_1, q}^*(z, \mathbf{r}_{2D}) \frac{\partial}{\partial q} u_{v; \kappa_2, q}(z, \mathbf{r}_{2D}) d\mathbf{r}_{2D} dz.$$

Using of the Schrödinger equation for the orthogonal Bloch wave functions  $\psi_{\kappa, q}(\mathbf{r})$  yields

$$U(q; d) = \frac{i\hbar^2}{E_{g; q, q} m_b} \int_0^d \int_{\mathbf{E}_2} \psi_{c; \kappa_1, q}^*(z, \mathbf{r}_{2D}) \frac{\partial}{\partial z} \psi_{v; \kappa_2, q}(z, \mathbf{r}_{2D}) d\mathbf{r}_{2D} dz. \quad (3.10)$$

Hence, in the long-wave limit the screened quasioone-dimensional electrostatic potential induced by a charge  $e_0$ , distributed with the density:

$$\rho^{\text{ext}}(z, \mathbf{r}_{2D}) = \frac{e_0}{\pi R^2 d} (\Theta[z + d/2] - \Theta[z - d/2]) (\Theta[r_{2D}] - \Theta[r_{2D} - R]), \quad R > 0,$$

$$\Theta(x - x_0) = \begin{cases} 0, & x < x_0, \\ 1, & x > x_0 \end{cases}$$

in accordance with (3.8) and (3.10), is given by the expression

$$\varphi(z) = \frac{8e_0 r_1}{\pi d^2} \int_0^\infty \frac{(1/k^2) \sin^2(kd/2r_1) \tilde{K}_0(k/r_1) \cos(kz/r_1)}{1 + g_d(kr_1/d) \sin(kd/2r_1) \tilde{K}_0(k/r_1)} dk \quad (3.11)$$

with

$$g_d = \left( \frac{e\hbar^2}{\pi r_1 m_b} \right)^2 \int_{-\pi/d}^{\pi/d} \frac{1}{E_{g; q, q}^3} \left| \left\langle \psi_{c; \kappa_1, q} \left| \frac{\partial}{\partial z} \right| \psi_{v; \kappa_2, q} \right\rangle \right|^2 dq. \quad (3.12)$$

According to equation (2.10) the dimensionless screening parameter  $g_d$  may be also written as:

$$g_d = \left( \frac{16e}{\hbar d r_1} \right)^2 m_b \int_0^{\pi/d} \frac{A_c^2(\kappa_1, q) A_v^2(\kappa_2, q)}{(\kappa_2^2(q) - \kappa_1^2(q))^5} \times \left| \left( 1 + \frac{Q_1(\kappa_1, q) Q_1(\kappa_2, q)}{Q_2^*(\kappa_1, q) Q_2(\kappa_2, q)} \right) \int_{\kappa_1}^{\kappa_2} Q_1(\kappa, q) d\kappa - \frac{Q_1(\kappa_1, q)}{Q_2^*(\kappa_1, q)} \int_{\kappa_1}^{\kappa_2} Q_2^*(\kappa, q) d\kappa - \frac{Q_1(\kappa_2, q)}{Q_2(\kappa_2, q)} \int_{\kappa_1}^{\kappa_2} Q_2(\kappa, q) d\kappa \right|^2 dq. \quad (3.13)$$

Note, that  $\kappa_1$  and  $\kappa_2$  are the implicit functions of  $q$  defined by (2.8) and (2.9), respectively.

It appears, that  $g_d$  calculated according to (3.13) for  $d$  varying in the interval  $[2.1a, 3a]$  are about  $10^{-6}$ .

## 4 Calculations. Discussion

Using equations (2.8) and (2.9) we obtained the band structure (see figure 1) and the electrons and holes effective masses for the linear, diatomic crystal for different values of the ratio  $j = d/a$  of its period  $d$  and the distance  $a$  between atoms in the unit cell. Besides, using wave equation (3.1) and potentials (3.2) and (3.11) we found the large-radius exciton energy spectrum in the crystal for the bare e-h interaction and e-h interaction screened by the bound electrons of the crystal. We present here results for the crystal with  $j \in [2.1, 3]$ . Contrary to the single-band metallic crystal with  $j = 2$ , the crystal with  $j = 2.1$  is already a wide-band-gap semiconductor.

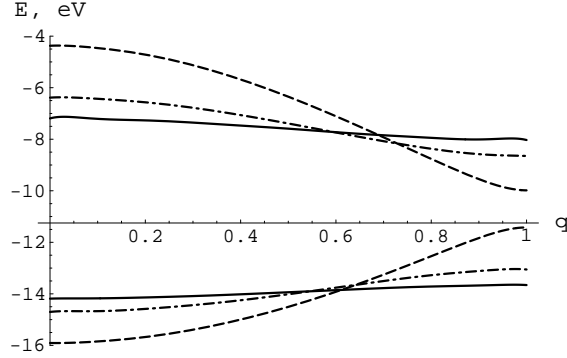


Figure 1: The band structure of the linear crystal with parameters:  $j = 2.1$  (dashed line),  $j = 2.5$  (dot-dashed line) and  $j = 3$  (solid line);  $q$  in units of  $\pi/d$ . The upper and lower bands correspond to equation (2.8) and (2.9), respectively

Table 1: Band gaps  $E_g$  and reduced effective masses  $\mu$  according to (2.8), (2.9); radii of the electrons and holes transverse localization  $r_1$  and  $r_2$ , respectively; screening parameter  $g_d$  according to (3.13) and the exciton binding energies  $\mathcal{E}$  of the even and odd series for the linear, diatomic crystal according to equation (3.1) with potential (3.2) for different values of the ratio  $j = d/a$

$j$	$E_g$ (eV)	$\mu$ ( $m_e$ )	$r_1$ (nm)	$r_2$ (nm)	$g_d$ ( $10^{-6}$ )	$\mathcal{E}_{0;\text{even}}$ (eV)	$\mathcal{E}_{1;\text{odd}}$ (eV)	$\mathcal{E}_{0;\text{even}}/E_g$
2.1	1.4422	0.041	0.070	0.0611	0.7235	-6.90	-0.5939	4.7845
2.3	3.3146	0.125	0.080	0.0569	2.4716	-8.9992	-2.0631	2.715
2.5	4.403	0.2199	0.088	0.0549	2.7036	-9.5352	-3.4812	2.1656
3	5.6281	0.5665	0.0994	0.0551	1.1206	-9.6588	-5.8421	1.7162

And the crystal with  $j = 3$  is almost a flat band semiconductor, but its electrons and holes at the energy gap ( $q = \pi/d$ ) still have the finite effective masses (these electrons and holes form the excitons in the crystal). The distance  $a$  we've chosen equal to the graphite in-plane parameter 0.142 nm. The ZRP interaction parameter  $\alpha = 11.01 \text{ nm}^{-1}$  corresponds to the ionization energy of isolated carbon atom ( $E_{\text{ion}} = 11.255 \text{ eV}$ ).

As one can see from table 1 the obtained from (3.13) dimensionless screening parameter  $g_d \ll 1$  for the all considered values of  $j$ . So, it turns out, that the screening of the e-h interaction potential by the bound electrons in the linear, diatomic crystal may be ignored. Therefore, only the binding energies of excitons with the unscreened interaction potential are listed in table 1.

Table 1 also shows that the ground-state exciton binding energies for the linear, diatomic crystals with any value of the ratio  $j$  are larger than the corresponding energy gaps. This effect has been also revealed in [6] and [10] for such quasio-one-dimensional structures as SWCNTs. Note, that according to the same calculations, but with the bare mass  $m_b = m_e$ , the ground-state exciton binding energy for the linear crystal in vacuum nevertheless appears significantly larger than the energy gap (even to a greater extent than in the case of  $m_b = 0.415 m_e$ ). This may lead to instability of the single-electron states at least in the vicinity of the energy gap with respect to formation of excitons. But as it was shown in [6] by the example of SWCNTs with the advent of a small number (about 0.1% of the band electrons number) of excitons in the crystal the additional screening effect, stipulated by a rather great polarizability of excitons in the longitudinal electric field, appears. This additional screening returns the lowest exciton binding energy into the energy gap and so blocks spontaneous transitions to the exciton states. Evidently, the shift of the forbidden band edges due to the transformation of some single-electron states into excitons results in some enhancement of the energy gap. For the linear crystal in a dielectric medium even with permittivity about  $\varepsilon \sim 2$  the ground-state exciton binding energy becomes smaller than the energy gap and none of the mentioned effects occurs.

In view of the above results we may conclude that the exciton contributions should appear in the optical spectrum of the linear, diatomic crystal and, most likely, in the optical spectrum of any quasio-one-dimensional isolated semiconductor in vacuum. Moreover, the small energy gap enhancement should take place for such semiconductors in vacuum with regard to those surrounded by a dielectric medium with  $\varepsilon \gtrsim 2$ .

## References

- [1] O'Connell M J *et al* 2002 Band gap fluorescence from individual single-walled carbon nanotubes *Science* **297** 593-6
- [2] Bachilo S M, Strano M S, Kittrell C, Hauge R H, Smalley R E and Weisman R B 2002 Structure-assigned optical spectra of single-walled carbon nanotubes *Science* **298** 2361-66
- [3] Ichida M, Mizuno S, Saito Y, Kataura H, Achiba Y and Nakamura A 2002 Coulomb effects on the fundamental optical transition in semiconducting single-walled carbon nanotubes: Divergent behavior in the small-diameter limit *Phys. Rev. B* **65** 241407(R)
- [4] Wang Z, Pedrosa H, Krauss T and Rothberg L 2006 Determination of the exciton binding energy in single-walled carbon nanotubes *Phys. Rev. Lett.* **96** 047403
- [5] Jorio A, Dresselhaus G and Dresselhaus M S (eds) 2008 *Carbon Nanotubes. Advanced Topics in the Synthesis, Structure, Properties and Applications* (Berlin, Heidelberg: Springer-Verlag)
- [6] Adamyan V M and Smyrnov O A 2007 Large radius excitons in single-walled carbon nanotubes *J. Phys. A: Math. Theor.* **40** 10519-33
- [7] Tishchenko S V 2006 Electronic structure of carbon zig-zag nanotubes *Low Temp. Phys.* **32** 953-6
- [8] Adamyan V and Tishchenko S 2007 One-electron states and interband optical absorption in single-wall carbon nanotubes *J. Phys.: Condens. Matter* **19** 186206
- [9] Albeverio S, Gesztesy F, Høegh-Krohn R and Holden H 1988 *Solvable Models in Quantum Mechanics. Texts and Monographs in Physics* (New York: Springer)
- [10] Bulashevich K A, Rotkin S V and Suris R A 2003 Excitons in single-wall carbon nanotubes *11th. Int. Symp. "Nanostructures: Physics and Technology" (St Petersburg, Russian Federation, June 23-28)*